

# Improving the Sensitivity of LISA

K. Rajesh Nayak<sup>†</sup>, A. Pai<sup>‡</sup>, S. V. Dhurandhar<sup>†</sup> and  
J-Y. Vinet<sup>‡</sup>

<sup>†</sup>Inter-University Centre for Astronomy and Astrophysics, Pune, India.

<sup>‡</sup>ILGA, Dept. Fresnel, Observatoire de la Cote d'Azur, BP 4229, 06304 Nice, France.

E-mail: [nayak@iucaa.ernet.in](mailto:nayak@iucaa.ernet.in),

[archana@obs-nice.fr](mailto:archana@obs-nice.fr), [sanjeev@iucaa.ernet.in](mailto:sanjeev@iucaa.ernet.in), [vinet@obs-nice.fr](mailto:vinet@obs-nice.fr)

**Abstract.** It has been shown in several recent papers that the six Doppler data streams obtained from a triangular LISA configuration can be combined by appropriately delaying the data streams for cancelling the laser frequency noise. Raw laser noise is several orders of magnitude above the other noises and thus it is essential to bring it down to the level of other noises such as shot, acceleration, etc. A rigorous and systematic formalism using the powerful techniques of computational commutative algebra was developed which generates in principle *all* the data combinations cancelling the laser frequency noise. The relevant data combinations form a first module of syzygies.

In this paper we use this formalism to advantage for optimising the sensitivity of LISA by analysing the noise and signal covariance matrices. The signal covariance matrix is calculated for binaries whose frequency changes at most adiabatically and the signal is averaged over polarisations and directions. We then present the extremal SNR curves for all the data combinations in the module. They correspond to the eigenvectors of the noise and signal covariance matrices. A LISA 'network' SNR is also computed by combining the outputs of the eigenvectors. We show that substantial gains in sensitivity can be obtained by employing these strategies. The maximum SNR curve can yield an improvement upto 70 % over the Michelson, mainly at high frequencies, while the improvement using the network SNR ranges from 40 % to over 100 %.

Finally, we describe a simple toy model, in which LISA rotates in a plane. In this analysis, we estimate the improvement in the LISA sensitivity, if one switches from one data combination to another as it rotates. Here the improvement in sensitivity, if one switches optimally over three cyclic data combinations of the eigenvector is about 55 % on an average over the LISA band-width. The corresponding SNR improvement increases to 60 %, if one maximises over the module.

## 1. Introduction

The proposed space-based mission of gravitational wave (GW) detection - the Laser Interferometric Space Antenna (LISA) - consists of three identical spacecrafts forming an equilateral triangle of side  $5 \times 10^6$  km following heliocentric orbits. LISA is thus a giant interferometric configuration with three arms which will give independent information on GW polarisations. The implementation of this huge Michelson interferometer is quite different from the ground based interferometers like LIGO, VIRGO etc. Unlike in the ground based interferometric detectors, it is not feasible to bounce the laser beams because of the large armlengths involved. A special Doppler tracking scheme is used to track the space crafts with laser beams. This exchange of laser beams between the three space-craft result in six Doppler data streams.

LISA sensitivity is limited by several noise sources. A major noise source is the laser phase noise which arises due to phase fluctuations of the master laser. Amongst the important noise sources, laser phase noise is expected to be several orders of magnitude larger than other noises in the instrument. The current stabilisation schemes estimate (this estimate may improve in the future) this noise to about  $\Delta\nu/\nu_0 \simeq 10^{-13}/\sqrt{Hz}$ , where  $\nu_0$  is the frequency of the laser and  $\Delta\nu$  the fluctuation in frequency. If the laser frequency noise can be suppressed then the noise floor is determined by the optical-path noise which causes fluctuations in the lengths of optical paths and the residual acceleration of proof masses resulting from imperfect shielding of the drag-free system. The noise floor is then at an effective GW strain sensitivity  $h \sim 10^{-21}$  or  $10^{-22}$ . Thus, cancelling the laser frequency noise is vital if LISA is to reach the requisite sensitivity. Since it is impossible to maintain equal distances between space-craft, cancellation of laser frequency noise is a non-trivial problem. Several schemes have been proposed to combat this noise. In these schemes [1, 2], the data streams are combined with appropriate time delays in order to cancel the laser frequency noise. In our earlier work [3], henceforth referred to as paper I, we had presented a systematic and rigorous method using commutative algebra which generates *all* the data combinations cancelling the laser frequency noise. These data combinations form a module over a polynomial ring, well known in the literature, as the *first module of syzygies*. We obtained the generators of this module and hence the entire set of relevant data combinations could be generated conveniently. More importantly, we note that this method is general and can be extended to space-missions with more than three spacecrafts.

In this paper we employ our previously set up formalism for two important applications: We compute the noise covariance matrix for LISA and obtain its eigenvectors and eigenvalues. The signal covariance matrix is computed for binaries whose frequency changes at most adiabatically (the monochromatic case is included) and for which the signal is averaged over polarisations and directions. Here adiabatic means that the signal response, the noise and hence the SNR change imperceptibly even if the GW source changes frequency during the observation time. Thus, even though the results are presented at each fixed frequency, the sources need not be strictly

monochromatic, and apply to a wider class of sources. The signal covariance matrix has the same eigenvectors as the noise covariance matrix which results in computational simplification. We show that the signal-to-noise (SNR) for any data combination in the module, then lies between an upper and a lower bound. The upper and lower bounds of the SNR are functions of frequency which are just the SNR curves of the eigenvectors. The extremisation - both maximisation and minimisation - of SNR is important for different purposes; maximisation is important for the detection and parameter estimation of a GW source, while minimisation is important for the purpose of distinguishing the GW confusion noise from the instrumental noise [4]. We further show that the bounding SNR curves have multiple intersections within the band-width of LISA ( $10^{-4} - 1$ ) Hz. The improvement of SNR of the upper-bound over the Michelson combination goes upto 70 % , but only at high frequencies  $\gtrsim 5$  mHz. At low frequencies  $\lesssim 5$  mHz, both have the same sensitivity. Since the eigenvectors are independent random variables, a ‘network’ SNR of independent detectors [5] can be constructed from the likelihood considerations which gives an improvement between  $\sqrt{2}$  and  $\sqrt{3}$  over the maximum of SNRs of the eigenvectors. The improvement over the Michelson combination is about 40 % at low frequencies  $\lesssim 3$  mHz and rises above 100 % at high frequencies. We may note that, some of our results are in agreement with independent and simultaneous calculations by Prince *et al* [6].

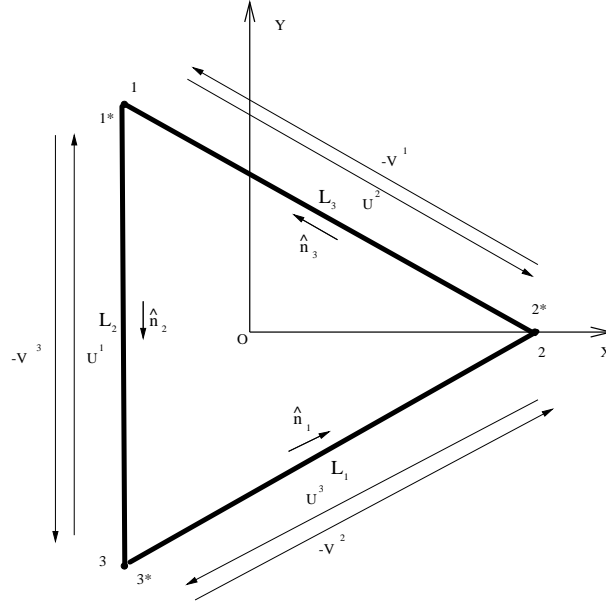
Tracking a GW source fixed on the celestial sphere for determining the SNR constitutes a non-trivial problem, which will require substantial analysis when writing codes. Here, we consider a simple toy model of LISA rotating in its own plane. Our goal is to obtain a rough estimate in the improvement of SNR by optimally switching from one data combination to another. We show that, if we implement this strategy, it is possible to improve the SNR by about 55 %.

## 2. The module of syzygies of time delayed data combinations

In this section, we briefly summarise the main results of paper I. It has been shown earlier in the literature [1, 2, 3], that the laser phase noise and the optical bench motion noise in the LISA can be suppressed by combining the six beams appropriately delayed across arms of the interferometer. The six data streams are labelled as  $U^i$  and  $V^i$ ,  $i = 1, 2, 3$ . The geometry of the LISA along with six laser beams is shown in the Figure -1. The beams  $U^i$  go clockwise while the  $V^i$  go counter-clockwise. There are also six other beams connecting the two optical benches on each space-craft (which are not shown in the figure). In the SNR analysis only the *difference* between these beams is important. These differences are denoted by  $Z^i$  where the index  $i$  corresponds to each space-craft labelled  $i$ .

In paper I, we have shown that *all* the data combinations which cancel the laser frequency noise and the bench motion noise form a module over a ring of polynomials in the three time delay operators  $E_i$ , where  $E_i, i = 1, 2, 3$  represent delay operators of the light travel time along the three arms with lengths  $L_i$ . Thus for the data stream  $x(t) : E_i x(t) = x(t - L_i)$  (the speed of light is set to unity); the operator  $E_i$  delays the

**Figure 1.** The LISA constellation consist of three spacecraft each carrying two optical bench systems  $i$  and  $i^*$ ,  $i = 1, 2, 3$ . They exchange six laser beams which are represented by  $U^i$  and  $V^i$  in the figure. The noise cancellation data combinations are obtained by appropriately delaying these six beams across the length of arms  $L_i$ .



data stream by amount  $L_i$ . For the LISA configuration  $L_i \sim 16.7$  seconds, corresponding to an arm-length of 5 million km. An important advantage of this formalism is that, one can generate the entire module from the generators; linear combinations of the generators with polynomial coefficients in the ring generate this noise cancellation module. Several sets of generators have been listed in paper I. Based on the physical considerations or for the purpose of computational convenience, we may choose one set over another. For the purpose of extremising the SNR, we choose the set of generators:  $\alpha, \beta, \gamma$  and  $\zeta$  (notation followed from [1, 2, 3]). The  $\alpha, \beta, \gamma$  are cyclic permutations of each other. This symmetry comes in useful when computing scalar products between them and also in diagonalising the noise, and signal covariance matrices defined in the next section. Following paper I, we list this generating set as 9-tuples of polynomials  $(p_i, q_i, r_i)$ . The polynomials  $(p_i, q_i, r_i)$  are polynomials in the variables  $E_i$  and act on the data streams  $(V^i, U^i, Z^i)$  respectively. The linear combination  $p_i V^i + q_i U^i + r_i Z^i$  cancels the laser frequency noise and optical bench motion noise when the 9-tuple  $(p_i, q_i, r_i)$  is an element of the module of syzygies. The generators of the module are given by:

$$\begin{aligned}
 \alpha &= (1, E_3, E_1 E_3, 1, E_1 E_2, E_2, -(1 + E_1 E_2 E_3), -(E_1 E_2 + E_3), -(E_1 E_3 + E_2)), \\
 \beta &= (E_1 E_2, 1, E_1, E_3, 1, E_2 E_3, -(E_1 E_2 + E_3), -(1 + E_1 E_2 E_3), -(E_1 + E_2 E_3)), \\
 \gamma &= (E_2, E_2 E_3, 1, E_3 E_1, E_1, 1, -(E_2 + E_1 E_3), -(E_1 + E_2 E_3), -(1 + E_1 E_2 E_3)), \\
 \zeta &= (E_1, E_2, E_3, E_1, E_2, E_3, -(E_1 + E_2 E_3), -(E_2 + E_1 E_3), -(E_3 + E_1 E_2)). \quad (1)
 \end{aligned}$$

We exhibit another set of generators  $\{X^{(A)}\}$  which was obtained from the software package Macaulay 2 [7]. They can be related to the above set of generators by:

$$\begin{aligned}
X^{(1)} &= E_3 \zeta - \gamma, \\
X^{(2)} &= \zeta, \\
X^{(3)} &= \alpha, \\
X^{(4)} &= \beta.
\end{aligned} \tag{2}$$

Note that these sets of generators are not linearly independent. In particular, the set of generators  $\{\alpha, \beta, \gamma, \zeta\}$  [1] obey the following condition :

$$(1 - E_1 E_2 E_3) \zeta = (E_1 - E_2 E_3) \alpha + (E_2 - E_1 E_3) \beta + (E_3 - E_1 E_2) \gamma. \tag{3}$$

When maximising the SNR in the Fourier space, this relation allows us to eliminate one of the generators at almost all frequencies, except when the product  $E_1 E_2 E_3 = 1$ . Note that  $E_1 E_2 E_3$  is just the total time-delay  $L_1 + L_2 + L_3$  around the LISA triangle. For the purposes of this paper, we assume that all the arms of LISA are of equal length *i.e.*  $L_1 = L_2 = L_3 = L$ . In the Fourier domain, *i.e.*,  $E_1 = E_2 = E_3 = E = e^{i\Omega L}$  and the operator polynomials become actual polynomials. One can then solve for  $\zeta$  in terms of  $\alpha, \beta, \gamma$ , *except* at the frequencies  $\Omega$ , when  $e^{3i\Omega L} = 1$ . Taking  $L \sim 5 \times 10^5$  km, the smallest such frequency  $f = \Omega/2\pi$  is  $\sim 20$  mHz. Thus,

$$\zeta = \frac{E}{1 + E + E^2} (\alpha + \beta + \gamma), \tag{4}$$

and can be effectively eliminated while extremising SNR, except at the singular frequencies. Since SNR computation can be successfully carried out for frequencies arbitrarily close to the singular frequencies, for the computation, the singularities do not seem to be important. In the analysis that follows, we use only the three generators  $\{\alpha, \beta, \gamma\}$ .

### 3. Strategies for improving the effective sensitivity of LISA

In this section, we show that the set of generators  $\{\alpha, \beta, \gamma\}$  can be combined into a new set, consisting of ‘orthogonal’ eigenvectors. The noise covariance matrix naturally defines a positive definite, non-degenerate bilinear form, which serves as a scalar product or a metric. Orthogonality between eigenvectors is defined in terms of this metric. Physically this means that the noises of the eigenvectors are uncorrelated with each other. The eigenvectors are easily obtained by diagonalising the noise covariance matrix. The averaged signal matrix that we consider here has the same form as the noise covariance matrix and consequently has the same eigenvectors. Thus this set of eigenvectors simultaneously diagonalises both matrices constituting the SNR and simplifies the analysis that follows. An important observation here is that the eigenvectors are independent observables. They represent therefore statistically independent detectors (so far as instrumental noises are concerned), and they can be treated as a network of detectors. Furthermore, they can be combined in a root mean square fashion to yield a ‘detector network statistic’ [5] to yield a much improved sensitivity.

### 3.1. The noise covariance matrix

Following the formalism in paper I, we define noise vectors in the Fourier domain  $N^{(I)}$ ,  $I = 1, 2, 3$  for each of the generators  $\{\alpha, \beta, \gamma\}$  respectively, over the 12 dimensional complex space  $\mathcal{C}^{12}$ ,

$$N^{(I)} = \left( \sqrt{S^{pf}}(2p_i^{(I)} + r_i^{(I)}), \sqrt{S^{pf}}(2q_i^{(I)} + r_i^{(I)}), \sqrt{S^{sh}}p_i^{(I)}, \sqrt{S^{sh}}q_i^{(I)} \right), \quad (5)$$

where  $S^{pf}(f)$  and  $S^{opt}(f)$  are power spectral densities (psd) of the proof mass residual motion and the optical path noise respectively. The polynomials  $(p_i^{(I)}, q_i^{(I)}, r_i^{(I)})$ , (now actual polynomials in the Fourier domain) corresponding to the generators  $\alpha$ ,  $\beta$  and  $\gamma$  are given in the equation (1). We take  $S^{pf}(f) = 2.5 \times 10^{-48} [f/1 \text{ Hz}]^{-2} \text{ Hz}^{-1}$  and  $S^{opt}(f) = 1.8 \times 10^{-37} [f/1 \text{ Hz}]^2 \text{ Hz}^{-1}$  following the literature [2]. It can be easily shown that for a given data combination, the norm of the noise vector represents its noise psd. The noise covariance matrix for the generators  $\{\alpha, \beta, \gamma\}$  is defined as  $\mathcal{N}^{(IJ)} = N^{(I)} \cdot N^{(J)*}$  and takes the simple form,

$$\mathcal{N}^{(IJ)} = \begin{bmatrix} n_d & n_o & n_o \\ n_o & n_d & n_o \\ n_o & n_o & n_d \end{bmatrix}. \quad (6)$$

We note that because of the cyclic symmetry, the diagonal elements  $N^{(I)} \cdot N^{(I)*}$  are equal to each other - denoted by  $n_d$ . Similarly, all the off-diagonal elements  $N^{(I)} \cdot N^{(J)*}$ , for  $I \neq J$  are also equal to each other and which we denote by  $n_o$ . This was the reason a generating set possessing symmetry properties was chosen in the first place. A matrix with this form has two degenerate eigenvalues. Thus, the eigenvalues of the noise covariance matrix are given by,

$$n_1 = n_2 = n_d - n_o \quad \text{and} \quad n_3 = n_d + 2n_o. \quad (7)$$

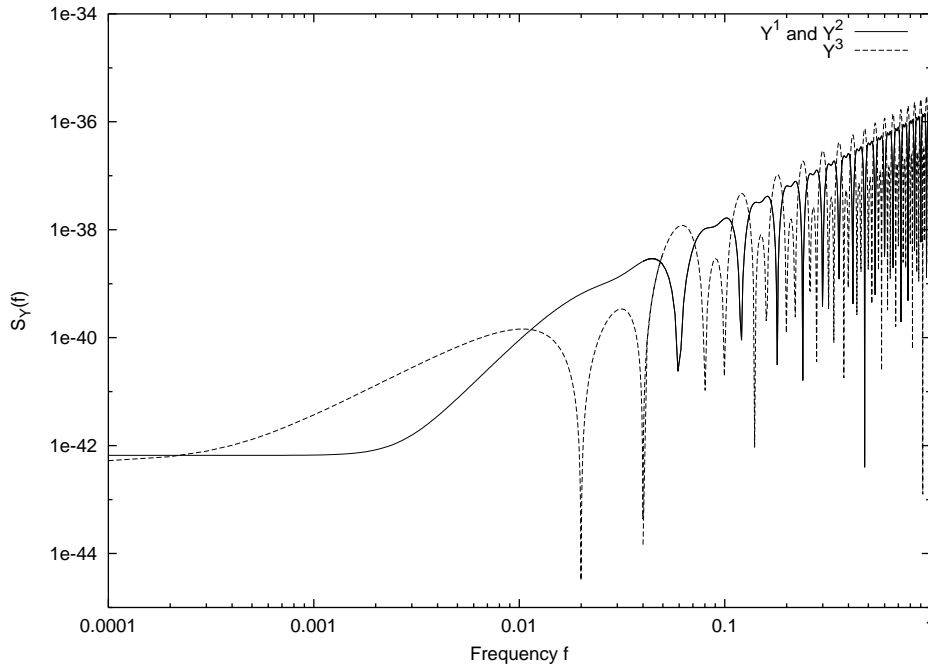
Since two of the eigenvalues are degenerate we need to systematically adopt a procedure for choosing the linearly independent and orthonormal set of eigenvectors. This choice is not unique. One such choice gives the following matrix  $\mathcal{M}$

$$\mathcal{M} = \begin{bmatrix} \frac{1}{\sqrt{6}} & \frac{1}{\sqrt{6}} & -\sqrt{\frac{2}{3}} \\ -\frac{1}{\sqrt{2}} & \frac{1}{\sqrt{2}} & 0 \\ \frac{1}{\sqrt{3}} & \frac{1}{\sqrt{3}} & \frac{1}{\sqrt{3}} \end{bmatrix}, \quad (8)$$

which diagonalises the noise matrix  $\mathcal{N}^{(IJ)}$ , that is  $\mathcal{M} \cdot \mathcal{N} \cdot \mathcal{M}^{-1}$  is diagonal, with eigenvalues as diagonal elements. The eigenvectors are:

$$\begin{aligned} Y^{(1)} &= \frac{1}{\sqrt{6}} (\alpha + \beta - 2\gamma), \\ Y^{(2)} &= \frac{1}{\sqrt{2}} (\beta - \alpha), \\ Y^{(3)} &= \frac{1}{\sqrt{3}} (\alpha + \beta + \gamma). \end{aligned} \quad (9)$$

We find that the data combination  $Y^{(3)}$  is proportional to the symmetric Sagnac combination  $\zeta$  and has the same SNR as that of  $\zeta$ .

**Figure 2.** Noise Spectra of combinations  $Y^{(l)}$ 


### 3.2. The signal covariance matrix

The response of a GW signal for a given data combination is computed in paper I. The response is conveniently expressed in the Fourier domain and is given by,

$$h(\Omega) = \sum_{i=1}^3 \left[ p_i \left( F_{V_{i,+}} h_+ + F_{V_{i,\times}} h_\times \right) + q_i \left( F_{U_{i,+}} h_+ + F_{U_{i,\times}} h_\times \right) \right] (\Omega). \quad (10)$$

Here,  $F_{V_{i,+/\times}}$  and  $F_{U_{i,+/\times}}$  are the antenna pattern functions. We note that the signal depends only on the first six entries ( $p_i, q_i$ ) of the 9-tuple describing a data combination. So while dealing with the signal response, we only consider the 6-tuple  $P = (p_i, q_i)$  of the 9-tuple describing a data combination. We apply this formalism to a binary source which may be adiabatically changing in frequency. The two GW amplitudes of such a source at frequency  $\Omega$  are given by,

$$h_+(\Omega) = \mathcal{A} \left( \frac{1 + \cos^2 \epsilon}{2} \cos 2\psi - i \cos \epsilon \sin 2\psi \right),$$

$$h_\times(\Omega) = \mathcal{A} \left( -\frac{1 + \cos^2 \epsilon}{2} \sin 2\psi - i \cos \epsilon \cos 2\psi \right).$$

Here, the parameters  $\epsilon$  and  $\psi$  describe the orientation of the source and enter into the expressions for the polarisation amplitudes. The direction of the source on the celestial sphere is given by the angles  $\theta$  and  $\phi$ . In order to organise the calculations, we also define the detector response 6-tuple as,

$$R = \left( F_{V_{i,+}} h_+ + F_{V_{i,\times}} h_\times, F_{U_{i,+}} h_+ + F_{U_{i,\times}} h_\times \right). \quad (11)$$

Both  $P$  and  $R$  will be considered as row vectors for the purposes of defining matrix products. In order to analyse the signal covariance matrix, it is useful to define a scalar product. For two data combinations  $P$  and  $Q$  (considered as row vectors), we define the scalar product as follows:

$$\ll P, Q \gg = P \cdot \mathcal{R} \cdot Q^\dagger, \quad (12)$$

where,  $\mathcal{R} = R^\dagger \cdot R$  is a Hermitian matrix of detector responses and the ‘dot’ denotes the matrix product. The norm of the vector  $P$  is then given by,

$$\|P\|^2 = \ll P, P \gg. \quad (13)$$

The norm of  $P$  is the GW response for the data combination described by  $P$ .

The signal covariance matrix for any generating set  $X^{(I)}$  (and corresponding  $P^{(I)}$ ) is then defined as,

$$\mathcal{H}^{(IJ)} = \langle h^{(I)} h^{(J)*} \rangle_{\epsilon\psi\theta\phi} = \langle \ll P^{(I)}, P^{(J)} \gg \rangle_{\epsilon\psi\theta\phi}, \quad (14)$$

where,  $h^{(I)} = P^{(I)} \cdot R^\dagger$  and the bracket  $\langle \rangle_{\epsilon\psi\theta\phi}$  represents the average over the polarisations and directions. Taking  $\alpha$ ,  $\beta$  and  $\gamma$  as the generators, the cyclic symmetry between them gives rise to a signal covariance matrix  $\mathcal{H}^{(IJ)}$  which has the same form as the noise covariance matrix  $\mathcal{N}^{(IJ)}$  given in equation (6). In this case the  $n_d$  and  $n_o$  are replaced by  $h_d = \langle h^{(I)} h^{(I)*} \rangle$  and  $h_o = \langle h^{(I)} h^{(J)*} \rangle$  respectively. Thus  $\mathcal{H}$  is diagonalised by the similarity transformation  $\mathcal{M}$  and has the *same* eigenvectors  $Y^{(I)}$ . The eigenvalues of  $\mathcal{H}^{(IJ)}$  are given by

$$h_1 = h_2 = h_d - h_o \quad \text{and} \quad h_3 = h_d + 2h_o. \quad (15)$$

This simultaneous diagonalisation of both signal and noise matrices is important from the point of extremisation of SNR. This forms the content of the next subsection. However, we may note that in the formalism developed by Prince *et al* [6], the optimisation is performed without averaging over the source directions and polarisations, which results in the GW source matrix of rank 1. Since, the source directions are not known in general, we average over these parameters which results in a signal matrix of rank 3.

### 3.3. Extremisation of SNR

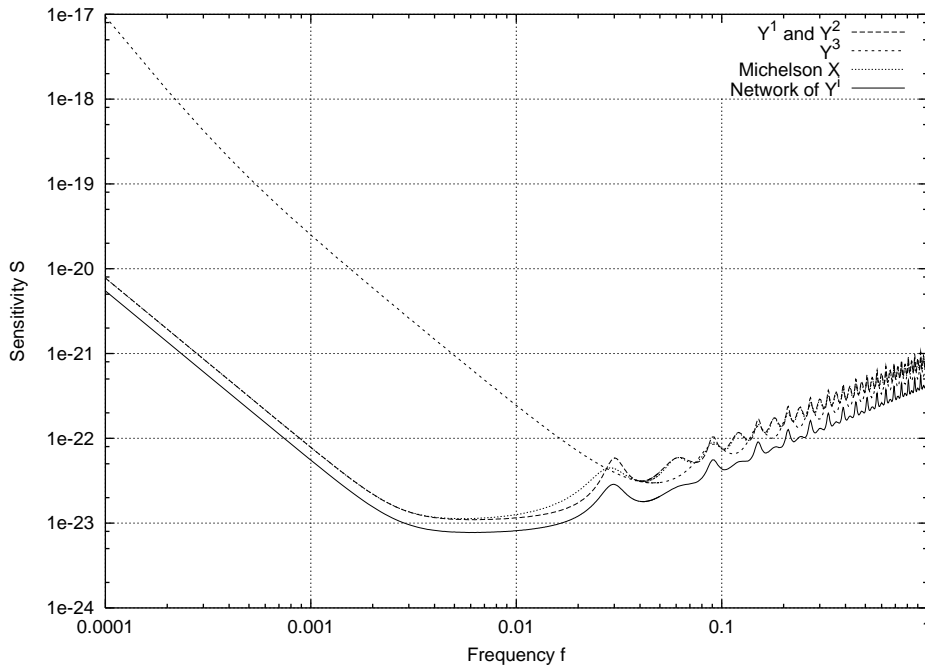
An arbitrary data combination can be written as  $Y = \alpha_{(I)} Y^{(I)}$ , where  $\alpha_{(I)}$  are polynomials in  $E$ . The SNR for this combination is given by,

$$SNR^2 = \frac{k_1 h_1 + k_3 h_3}{k_1 n_1 + k_3 n_3}, \quad (16)$$

where,  $k_1 = |\alpha_1|^2 + |\alpha_2|^2$  and  $k_3 = |\alpha_3|^2$ , and the ranges of  $k_1, k_3$  are from 0 to  $\infty$ . The simplicity of this expression is because of using the new set of the orthogonal generators  $Y^{(I)}$ . It enables us to easily solve the extremisation problem. The maximum and the minimum of this expression is governed by the quantity  $\eta$  where,

$$\eta(f) = \frac{SNR_{(1)}^2}{SNR_{(3)}^2} = \frac{h_1/n_1}{h_3/n_3}, \quad (17)$$

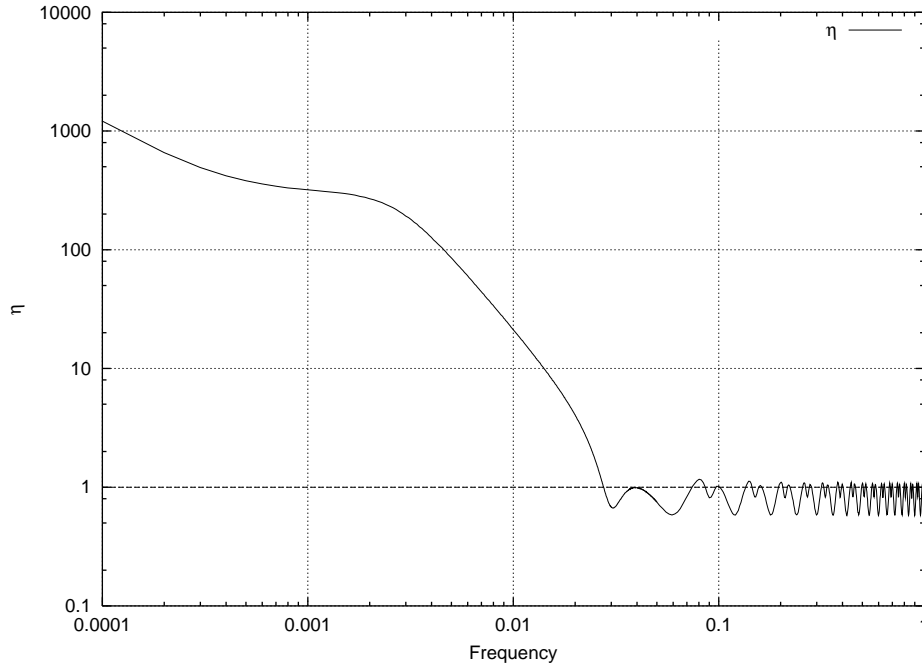
**Figure 3.** Log Log plot of sensitivity  $S$ , curve as function of  $f$  after averaging over polarisation and source directions for a observation period of one year and  $SNR = 5$ .



where  $SNR_{(I)}$  denotes the SNR of  $Y^{(I)}$ . When  $\eta(f) \neq 1$ , the SNR is a strictly monotonic function of the ratio  $k_1/k_3$ . If  $\eta(f) > 1$  then the SNR of the generator  $Y^{(1)}$  or  $Y^{(2)}$  is greater than that of  $Y^{(3)}$ . Then for these frequencies  $Y^{(1)}$  or  $Y^{(2)}$  (or any linear combination of them) yields the maximum SNR while  $Y^{(3)}$  yields minimum SNR. When  $\eta(f) < 1$ , the opposite is true:  $Y^{(1)}$  or  $Y^{(2)}$  (or any linear combination of them) yield the minimum SNR while  $Y^{(3)}$  yields maximum SNR. The remaining case, when  $\eta(f) = 1$  all the  $Y^{(I)}$  have the same SNR. Since the extremum values of SNR are only attained by the eigenvectors, the corresponding SNR curves constitute the bounding curves for any linear combination of  $Y^{(I)}$  s. So our results determine the limiting sensitivities of data combinations cancelling laser frequency noise and optical bench motion noise. It is interesting to note that at the frequencies where the bounding curves intersect, *all* the data combinations belonging to the module have the same SNR.

In the lower frequency range ( $f \lesssim 15 \text{ mHz}$ ), the combination  $Y^{(3)}$  (same as that of the combination  $\zeta$ ) has a very low sensitivity to the gravitational wave signal and the generators  $Y^{(1)}$  (or  $Y^{(2)}$ ) has maximum sensitivity to the signal. However, at high frequencies, the sensitivity curves of  $Y^{(1)}$  and  $Y^{(3)}$  intersect at several frequencies eg.  $\sim 27 \text{ mHz}$ ,  $39 \text{ mHz}$  etc. While computing  $\mathcal{H}^{(IJ)}$  and the average sensitivity, we assume a uniform distribution of sources over polarisations and source directions in the sky. Averaging over the polarisations is performed analytically and the averaging over source directions performed using the Monte Carlo method. The sensitivity,  $S$  is defined following the reference [8],  $S = 5 \sqrt{\frac{B}{SNR}}$ , here,  $B = \frac{1}{T}$  and  $T$  is the observation time which we take to be one year. In the Figure 3, we show the plots of  $S$  for the basis elements

**Figure 4.** Plot of parameter  $\eta$  as a function of  $f$ . The points  $\eta = 1$  correspond to the frequencies at which all the data combinations have the same SNR.  $\eta > 1$  corresponds to the region in which data combination  $Y^{(1)}$  and  $Y^{(2)}$  are more sensitive than  $Y^{(3)}$  and vice versa.



$Y^{(I)}$ , for comparison, we also plot the sensitivity for the Michelson combination  $X$ . In the Figure 4, we plot the ratio  $\eta$  as a function of the frequency  $f$ . The points at which  $\eta$  intersects the line  $y = 1$  corresponds to the points where all the data combinations in the module have the same value of SNR.

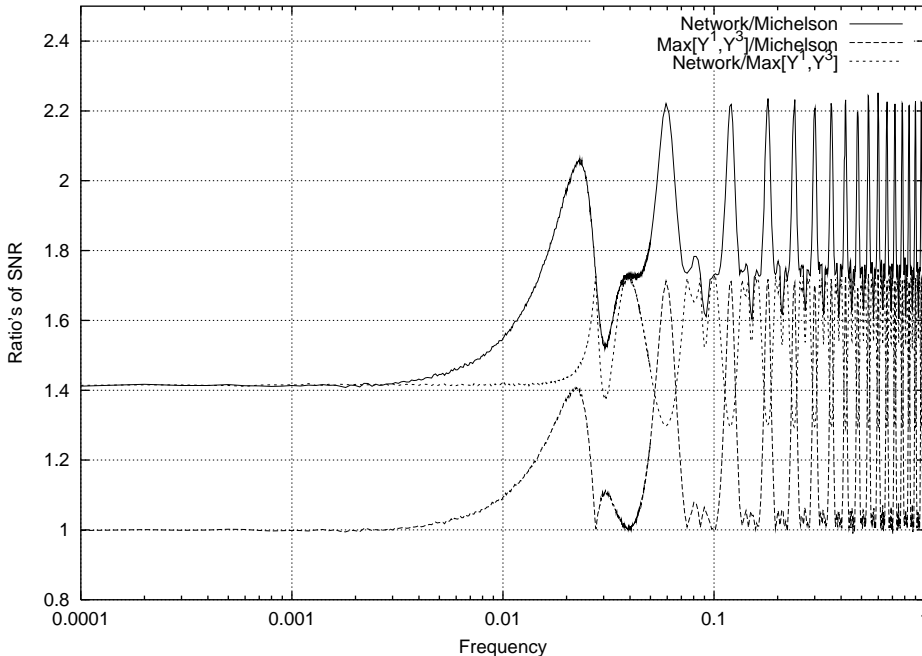
### 3.4. Operating LISA in a network mode

In the preceding sections, we have shown that either  $Y^{(1)}$ ,  $Y^{(2)}$  or  $Y^{(3)}$  maximise the SNR and they are orthogonal *i.e.* they are independent random variables. The sensitivity of LISA can be further improved because, each of these generators can be realized as independent gravitational wave detectors. Here we obtain the network SNR by taking  $Y^{(I)}$  as independent outputs of a network of three detectors. We assume that the underlying noise is Gaussian [5] and the  $Y^{(I)}$  follow the standard normal distribution.

As shown in [5], if the noise of the individual detectors is uncorrelated then the network likelihood ratio is just the product of individual likelihood ratios; the log network likelihood ratio is the sum of the individual log likelihood ratios. Moreover, if the noise in the individual detectors is Gaussian, the surrogate statistic of the network, yields the network SNR as,

$$SNR_{network}^2 = \sum_{I=1}^3 SNR_{(I)}^2 = 2 \frac{h_1}{n_1} + \frac{h_3}{n_3}. \quad (18)$$

**Figure 5.** Plots showing the relative improvements (ratios) of SNRs for the three cases: (i) Network SNR over the Michelson data combination (solid line). (ii) Network SNR over the maximum of  $\text{Max}[Y^{(1)}, Y^{(3)}]$  (dotted line). (iii)  $\text{Max}[Y^{(1)}, Y^{(3)}]$  over the Michelson (dashed line). Here  $\text{Max}[Y^{(1)}, Y^{(3)}]$  is the maximum of the SNR of  $Y^{(1)}$  and  $Y^{(3)}$  over the bandwidth of LISA.



The corresponding sensitivities are shown in the Figure 3. At low frequencies  $f \lesssim 15$  mHz, the improvement of the network SNR over the maximum of  $Y^{(I)}$  is slightly greater than  $\sqrt{2}$ . This is because at low frequencies the data combination  $Y^{(3)}$  is not very sensitive in comparison with  $Y^{(1)}$ . The best improvement in the relative SNR is achieved at frequencies where all the data combinations are equally sensitive, that is, when  $\eta = 1$ . A gain of a factor of  $\sqrt{3}$  is achieved at these points. In the Figure 5, we have plotted the relative improvements in the network SNR with respect to the Michelson combination and the maximum of  $Y^{(1)}$  and  $Y^{(3)}$ .

#### 4. SNR maximisation for a toy model of the LISA triangle rotating in a plane

The LISA configuration consists of three spacecraft which orbit with complex trajectories in order to maintain a stable triangular configuration in an heliocentric orbit [8]. We note that the transfer functions of the beams  $U^i, V^i$  are computed in the frame of LISA. Hence, a given GW source which is fixed on the celestial sphere will appear to follow a complex trajectory in this frame. This motion is the superposition of two rotations. One is just a rotation of the LISA triangle in its own plane. The other is its motion around the Sun in which the configuration follows the earth in an earthlike orbit. The period of the two rotations is identical and is one year in duration. Since

LISA has a non-uniform directional response, it is a non-trivial problem to track the apparent motion of a ‘fixed’ GW source in the LISA frame and then compute its SNR.

We consider a toy model in which only one motion is taken into account, which is the rotation of LISA about an axis orthogonal to the plane containing the three spacecraft. We ignore the other motion of LISA around the Sun for simplicity. Following paper I, we choose the  $X - Y$  plane to coincide with the plane formed by the three spacecraft constituting the LISA triangle. The origin is chosen at the centre of the equilateral triangle (for computing the response, we take all the arms to be of equal length). The positive  $X$ -axis passes through spacecraft 2. Figure 1 shows how the  $X - Y$  axes have been chosen. The  $Z$ -axis is orthogonal to this plane with the positive direction given by the right-handed convention. Under these assumptions, the source would appear to move in the sky in a circular trajectory about the  $Z$ -axis with a period of one year. In terms of polar coordinates  $(\theta, \phi)$ , the motion of such a source is uniform along  $\phi$  with a constant value of  $\theta$ . If one tracks a source with a single data combination, say  $Y^{(1)}$ , because the directional sensitivity of  $Y^{(1)}$  is non-uniform, it does not track the source optimally. Figure (6) displays the 3-dimensional sensitivity plots of  $Y^{(1)}$  and  $Y^{(2)}$  as a function of the angles  $(\theta, \phi)$  for a monochromatic source at the GW frequency of 1 mHz and the signal uniformly averaged over the polarisations (this average is computed analytically). It is obvious from these plots that the sensitivity is a highly non-uniform function of source direction. We consider here the case when the source with GW frequency 1 mHz lies in the plane of the LISA triangle, that is, the GW source lies in the  $\theta = \frac{\pi}{2}$  plane. We choose this value because, in the plane of LISA, the variations in the sensitivity are maximum for the combinations  $Y^{(1)}$  and  $Y^{(2)}$ . From the Figures (6) and (7), we note that the generators  $Y^{(I)}$  have zero sensitivity at few values of  $\phi$ . This implies that no single data combination, even if it is a linear combination of these, can give optimal sensitivity. To obtain best results, one needs to maximise the SNR over the linear combinations  $\alpha_{(I)}Y^{(I)}$ .

We analyse two strategies for optimising the sensitivity:

- (a) We consider the cyclic permutations of  $Y^{(1)}$  and compute the maximum sensitivity using these three data combinations.
- (b) We take the maximum of the linear combinations  $\alpha_{(I)}Y^{(I)}$  where  $\alpha_{(I)}$  are complex numbers. At each value of  $\phi$ , a different linear combination of  $Y^{(I)}$  is optimal. Thus the  $\alpha_{(I)}$  for which the SNR is maximised are, in general, functions of  $\phi$ .

The results of these analyses are described in Figure (9). For the strategy (a), the improvement in sensitivity averaged over  $\phi$  is  $\sim 49\%$ ; while for the strategy (b), the improvement in sensitivity averaged over  $\phi$  is  $\sim 59\%$ . In addition Figure (8) shows the plots of  $\alpha_{(I)}$  as function of  $\phi$ , which maximise the SNR.

The strategy (a) does not give the best SNR as it maximises the response over only a set of three data combinations. On the other hand, strategy (b) maximises the SNR over the module and is therefore superior. It is interesting to note that the maximised SNR is constant as a function of  $\phi$  and is the same as the SNR of  $Y^{(1)}$  maximised over

**Figure 6.** Plot of  $\log S$ , of the  $Y^{(1)}$  and  $Y^{(2)}$ , are displayed in (a) and (b) respectively, as a function of  $\theta$  and  $\phi$  for  $f = 1 \text{ mHz}$  and  $\text{SNR}=5$  over a observation period of one year.

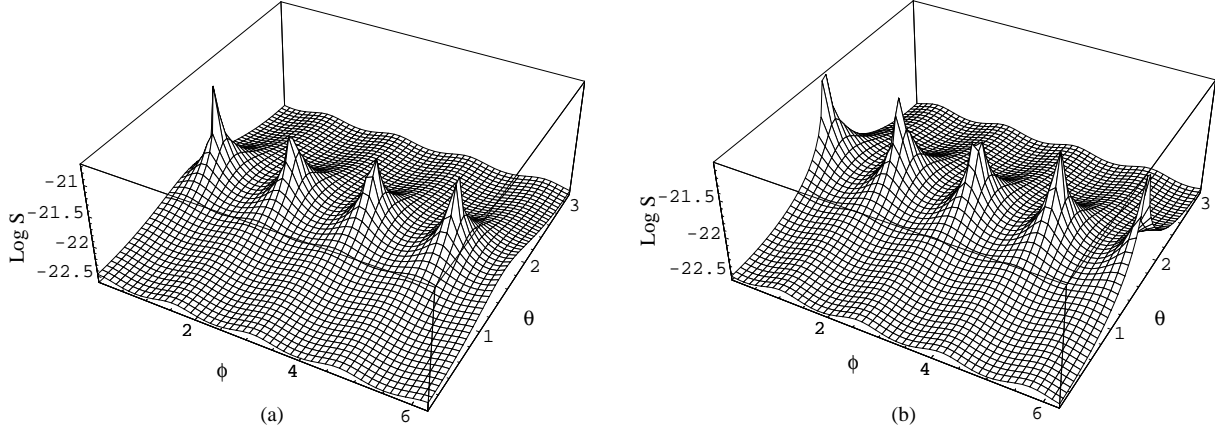
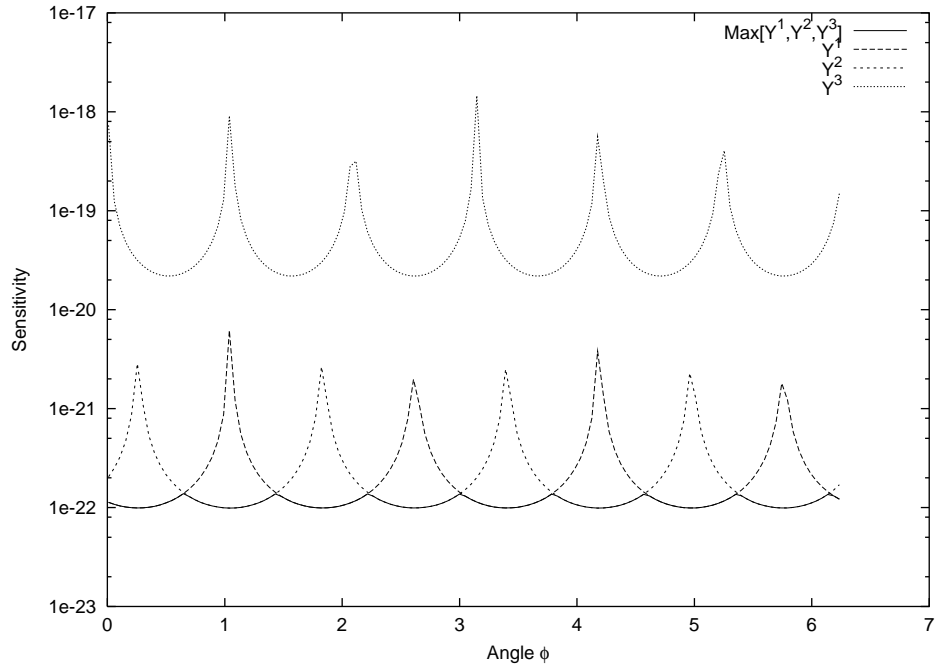


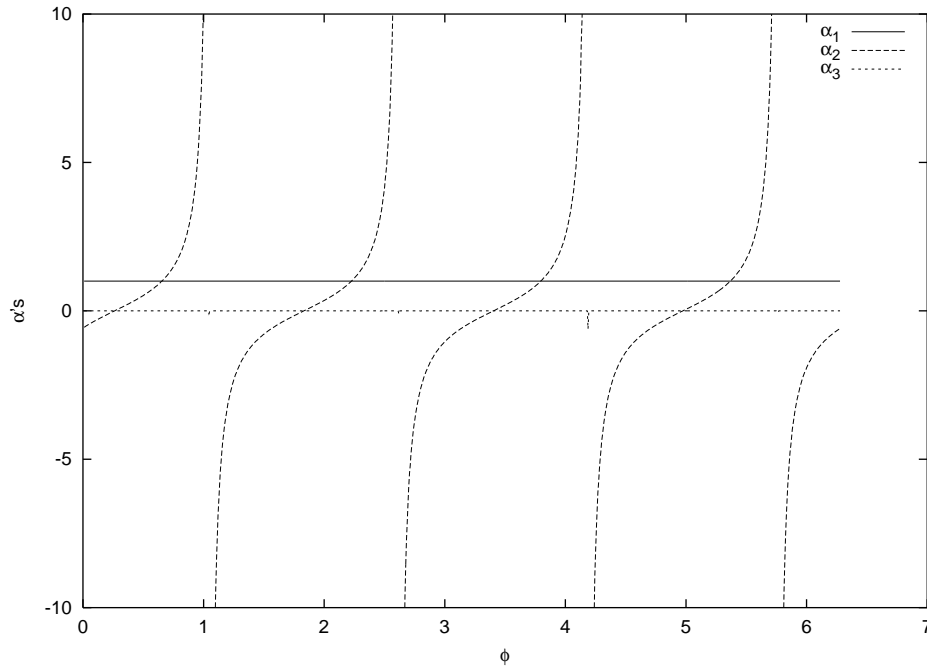
**Figure 7.** Plot of sensitivity as a function angle  $\phi$  at  $\theta = \frac{\pi}{2}$  and  $f = 1 \text{ mHz}$  after averaging over the polarisations.



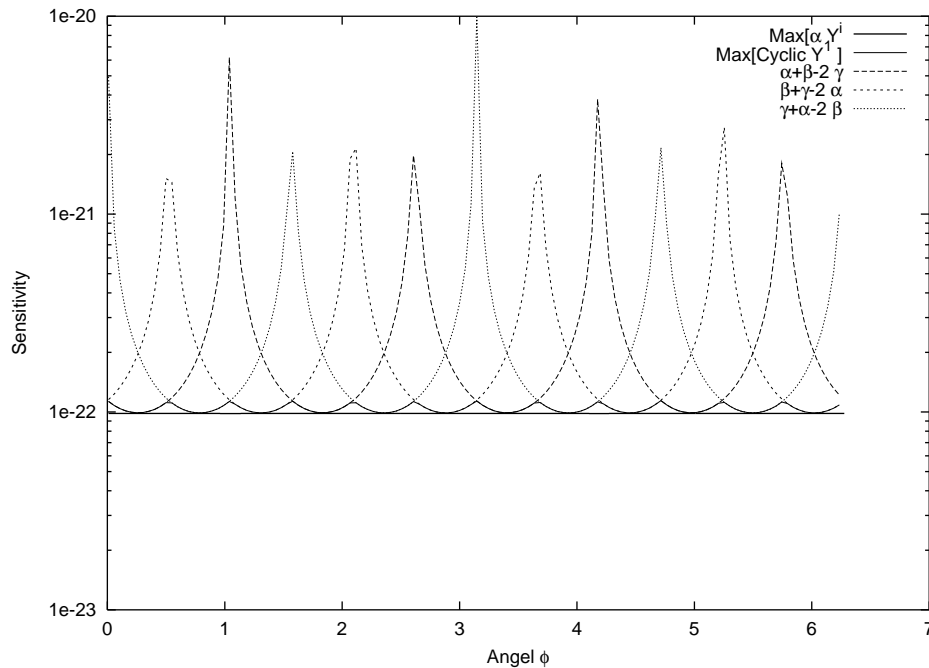
$\phi$ . We remark that the strategy (b) gives only marginal improvement over strategy (a), and also strategy (a) is easier to implement requiring relatively fewer computations.

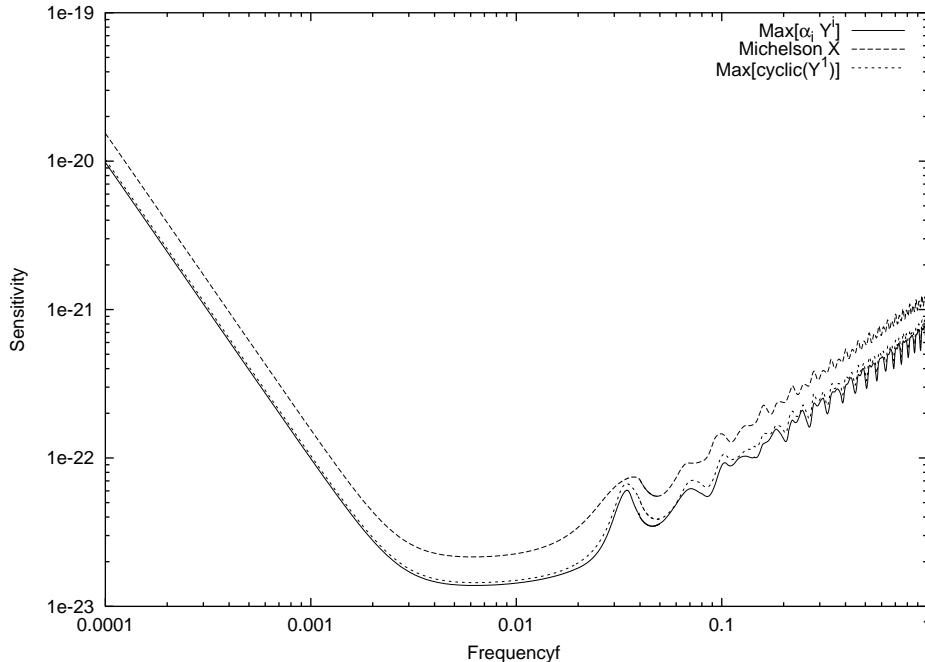
As seen for a GW source with a frequency of 1 mHz, strategy (b) gives a constant value for the maximum sensitivity over  $\phi$  (see Figure (9)). Thus the maximum sensitivity is independent of  $\phi$  for a given frequency. We further extend this analysis to other frequencies over the band-width of LISA, and obtain analogous results to the case of 1 mHz. This maximum sensitivity however depends on the frequency. In Figure (10),

**Figure 8.** The coefficients  $\alpha_{(I)}$  maximising the SNR of the combination  $\alpha_{(I)}Y^{(I)}$  are plotted as functions of  $\phi$  for the frequency 1 mHz and  $\theta = \pi/2$ .



**Figure 9.** Sensitivity curves for the toy model of LISA are given as functions of  $\phi$  at  $f = 1 \text{ mHz}$ . The curves represented by broken lines correspond to the  $Y^{(1)}$  and its cyclic permutations. The solid line curves represent the sensitivities for the two strategies: (a) taking the maximum of  $Y^{(1)}$  and its cyclic permutations (thin solid line); (b) taking maximum over the linear combinations of  $Y^{(I)}$ ,  $I = 1, 2, 3$  (thick solid line).



**Figure 10.** Plot of sensitivity  $S$  as a function of frequency, for the toy model.

we present the maximum sensitivity curves as functions of frequency. For comparison, we perform analogous computations for the Michelson data combination  $X$  and the maximum of the cyclic permutations of  $Y^{(1)}$ . In all these cases, the GW amplitude is first averaged over the polarisations and then for a fixed frequency, the sensitivity as a function of  $\phi$  is computed and then averaged over  $\phi$ . Finally, this exercise is carried out for frequencies across the LISA band-width.

The 1 mHz case is representative of the low frequency regime  $\lesssim 3$  mHz where the improvement in sensitivity is about 49 % for strategy (a) and 59 % for strategy (b). These improvements scale up at higher frequencies at say,  $\sim 15$  mHz, to 56 % and 67 % , respectively, for the two strategies (a) and (b).

## 5. conclusion

In this paper, we have employed our previously set up formalism from paper I for two important applications:

The first application is the extremisation of SNR. We have considered binaries as GW sources whose frequencies change at most adiabatically (monochromatic sources are included), that is, even if the frequency changes during the observation time, the change in SNRs under consideration is insignificant. The signal covariance matrix has been computed for which the signal is averaged over polarisations and directions. We have then computed the noise covariance matrix for LISA and obtained its eigenvectors and eigenvalues. This matrix has the same eigenvectors, resulting in calculational simplification. We have shown that the SNR for any data combination in the module,

lies between the upper and lower bounds which are determined by the eigenvectors of both matrices. We have further shown that the bounding SNR curves of the eigenvectors have multiple intersections within the band-width of LISA -  $10^{-4}$  - 1 Hz. We have obtained the following results for the improvement in SNR: The improvement of SNR of the upper-bound over the Michelson combination goes upto 70 % , at high frequencies  $\gtrsim 5$  mHz, however, at low frequencies  $\lesssim 5$  mHz, both have the same sensitivity. Since the eigenvectors are independent random variables, a ‘network’ SNR of independent detectors [5] has been constructed from likelihood considerations which gives an improvement between  $\sqrt{2}$  and  $\sqrt{3}$  over the maximum of SNRs of the eigenvectors. The improvement of the network SNR over the Michelson combination is about 40 % at low frequencies  $\lesssim 3$  mHz and rises above 100 % at high frequencies.

The second application is a simple toy model of LISA rotating in its own plane. For this model we estimated the improvement of SNR by optimally switching from one data combination to another. We have shown that, if this strategy is used, it is possible to improve the SNR by about 55 % on an average over the band-width of LISA. We also show that if we instead maximise over the module, the SNR improves by about 60 % on an average over the LISA band-width. These improvements are obtained using just one data combination, namely, the eigenvector  $Y^{(1)}$ . The SNR improvement in both cases is larger at higher frequencies  $\gtrsim 10$  mHz than at low frequencies.

## Acknowledgments

The authors would like to thank B. F. Schutz for in depth discussions which provided valuable physical insights and for suggesting the toy model scenario. The authors would like to thank T. Prince and M. Tinto for useful discussions.

- [1] J. W. Armstrong, F. B. Eastabrook and M. Tinto *Ap. J.*, **527**, 814(1999).
- [2] F. B. Estabrook, M. Tinto and J.W. Armstrong, *Phys. Rev.*, **D 62**, 042002(2000).
- [3] S. V. Dhurandhar, K. Rajesh Nayak, J-Y. Vinet, *Phys. Rev.*, **D 65** , 102002(2002).
- [4] M. Tinto and J. W. Armstrong, *Phys. Rev.* **D 59**, 102003 (1999).
- [5] S. Bose, S. V. Dhurandhar and A. Pai, *Pramana*, **53**, 1125-1136 (1999).
- [6] T. A. Prince, M. Tinto, S. L. Larson and J.W. Armstrong , *gr-qc/0209039*, <http://arxiv.org/> , (2002).
- [7] Macaulay2 software by D. R. Grayson and M. E. Stillman, <http://www.math.uiuc.edu/Macaulay2/>.
- [8] P. Bender *et al.* "LISA: A Cornerstone Mission for the Observation of Gravitational Waves", System and Technology Study Report ESA-SCI(2000) 11, 2000.